Scand J Med Sci Sports 2015: ●●: ●●–●●
doi: 10.1111/sms.12625

SCANDINAVIAN JOURNAL OF
MEDICINE & SCIENCE
IN SPORTS

Proximal hamstring morphology and morphometry in men: an anatomic and MRI investigation

R. N. Storey[1], G. R. Meikle[2], M. D. Stringer[1], S. J. Woodley[1]

[1]Department of Anatomy, University of Otago, Dunedin, New Zealand, [2]Radiology Department, Dunedin Public Hospital, Dunedin, New Zealand
Corresponding author: Stephanie J. Woodley, Department of Anatomy, University of Otago, PO Box 913, Dunedin 9054, New Zealand. Tel.: +64 3 479 7353, Fax: +64 3 479 7254, E-mail: stephanie.woodley@anatomy.otago.ac.nz

Accepted for publication 25 October 2015

The proximal musculo-tendinous junction (MTJ) is a common site of hamstring strain injury but the anatomy of this region is not well defined. A morphometric analysis of the proximal MTJs of biceps femoris long head (BFlh), semitendinosus (ST), and semimembranosus (SM) was undertaken from dissection of 10 thighs from five male cadavers and magnetic resonance imaging of 20 thighs of 10 active young men. The length, volume, and cross-sectional area of the proximal tendon, MTJ and muscle belly, and muscle-tendon interface area were calculated. In both groups, MTJs were reconstructed three-dimensionally. The proximal tendons and MTJs were expansive, particularly within SM and BFlh. Morphology varied between muscles although length measurements within individual muscles were similar in cadavers and young men. Semimembranosus had the longest proximal tendon (cadavers: mean 33.6 ± 2.0 cm; young men: mean 31.7 ± 1.6 cm) and MTJ (>20 cm in both groups) and the greatest muscle-tendon interface area, followed by BFlh and ST. Mean muscle belly volumes were more than three times greater in young men than elderly male cadavers ($P < 0.001$). These unique morphometric data contribute to a better understanding of hamstring anatomy, an important factor in the pathogenesis of hamstring strain injury.

Hamstring strains represent one of the most common injuries in sports, particularly those involving high-speed running, kicking, and changes in direction, such as Australian football and soccer (Petersen et al., 2010; Eirale et al., 2013; Orchard et al., 2013). Recurrent injury affects between 14% and 63% of individuals (Gibbs et al., 2004; Petersen et al., 2010; Storey et al., 2012; Orchard et al., 2013) and often results in a prolonged recovery and prevents a timely return to pre-injury activities (Gibbs et al., 2004).

Muscle-tendon architecture is an important consideration in multifactorial models of hamstring strain, alongside other parameters such as muscle flexibility, strength, and fatigue (Mendiguchia et al., 2012). It is well documented that the long head of biceps femoris (BFlh) is injured more frequently than the medial hamstring muscles (Slavotinek et al., 2002; Koulouris & Connell, 2003; Askling et al., 2007a; Petersen et al., 2014), and that most strains occur proximally (De Smet & Best, 2000; Koulouris & Connell, 2003; Askling et al., 2007a). Furthermore, it is recognized that morphological factors influence the time taken to return to pre-injury levels of function, namely the specific muscle(s) injured (Connell et al., 2004; Askling et al., 2007a,b), as well as the location (Askling et al., 2000, 2006, 2007a) and extent (Slavotinek et al., 2002; Connell et al., 2004; Gibbs et al., 2004) of injury within the muscle-tendon complex.

A number of studies have examined the morphology of the hamstring muscles (Wickiewicz et al., 1983; Garrett et al., 1989; Seidel et al., 1996; Chleboun et al., 2001; Woodley & Mercer, 2005; Evangelidis et al., 2015; van der Made et al., 2015). However, only a few have investigated the anatomy of the proximal muscle-tendon complex (Woodley & Mercer, 2005; Kellis et al., 2009; Battermann et al., 2011; Sato et al., 2012; Evangelidis et al., 2015; van der Made et al., 2015) which is surprising given that strain injuries most commonly occur adjacent to this site (Slavotinek et al., 2002; Koulouris & Connell, 2003; Askling et al., 2007a; Storey et al., 2012). The length and expansive intramuscular arrangement of the proximal hamstring tendons have been described (Woodley & Mercer, 2005; Miller et al., 2007; Kellis et al., 2009; van der Made et al., 2015), but these anatomical data were derived from linear measurements in cadavers. A recent study examined the size of the proximal BFlh aponeurosis using magnetic resonance imaging (MRI) (Evangelidis et al., 2015);

however, little attention has been directed at morphometric parameters such as proximal tendon volume and the relationship between muscle-tendon interface area and muscle volume. A clearer understanding of proximal hamstring morphology might contribute to an increased understanding of hamstring strain injuries.

The aim of this study was to examine the detailed morphology and morphometry of the proximal hamstring tendons and musculo-tendinous junctions (MTJs) in men, using a combination of cadaver dissection and MRI.

Methods

Cadaver study

The hamstring muscles were investigated in 10 lower limbs from five embalmed (ethanol-based fixative) male cadavers (mean age 74.6 years) bequeathed under the New Zealand Human Tissue Act (2008). Skin, superficial and deep fascia, gluteus maximus and neurovascular bundles were removed from the posterior thigh and gluteal region to reveal the hamstring muscles.

Muscle and tendon morphometry

In addition to morphological observations, measurements were taken of the hamstrings *in situ* (RS), using digital calipers (point digital sliding calipers SC02; Tresna, Guilin, P.R. China) and a flexible tape measure (if greater than 10 cm). The prominent tubercle on the lateral aspect of the medial portion of the ischial tuberosity was used as the proximal landmark (Woodley & Mercer, 2005). Total muscle length was defined as the distance between this landmark and the inferior margin of the fibular head (BFlh) or the point on the tibia where the medial condyle begins to flare laterally (semitendinosus [ST] and semimembranosus [SM]). Muscle belly length, proximal tendon length, free tendon length, and MTJ length were recorded (Fig. 1) (Woodley & Mercer, 2005; Askling et al., 2007b).

The hamstring muscles were then resected *en bloc* from their insertions and embedded in commercial jelly (Leiner Davis Gelatin, Christchurch, New Zealand) at four times its normal concentration (100 g/l). A black base layer of jelly was

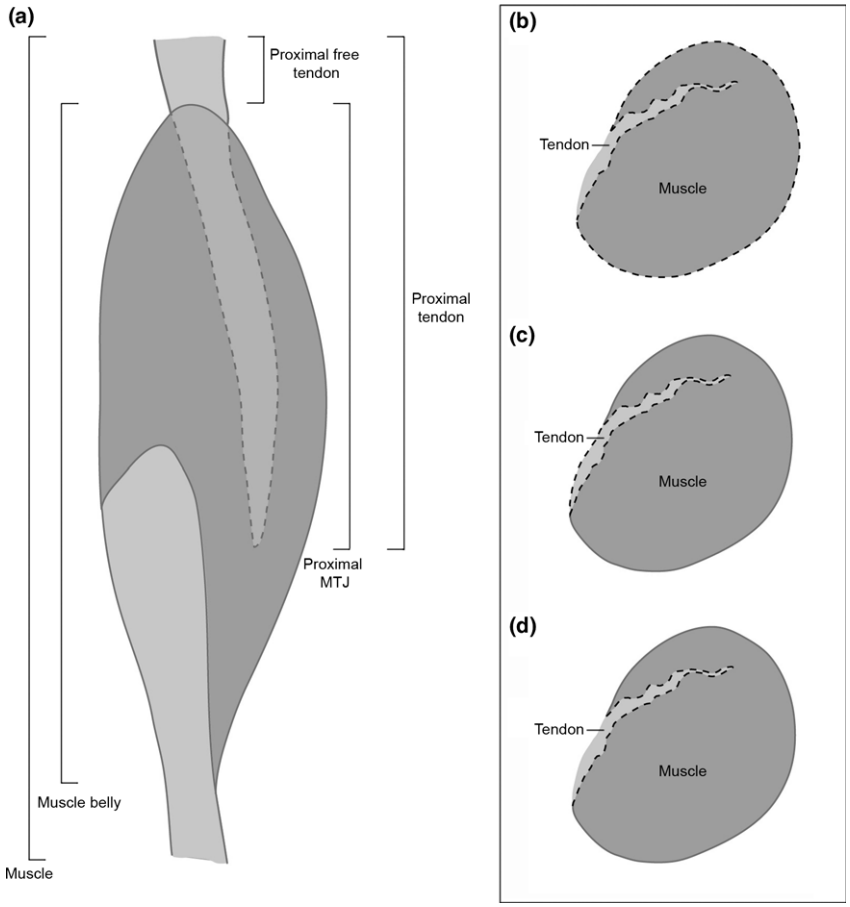

Fig. 1. Schematic of measurements obtained from cadaver specimens and magnetic resonance images of young active males. (a) Depictions of length measurements taken with the hamstring muscles *in situ* following dissection, for cadaver serial sections and axial magnetic resonance images; (b) Muscle cross-sectional area; (c) Tendon cross-sectional area; (d) Muscle-tendon interface area (cadaver specimens only). The dashed lines in B–D represent the area measured. Cross-sectional area data were used to calculate total muscle and tendon volume using the following formula: Volume (cm^3) = ΣAd, where A is the cross-sectional area of muscle or tendon and d is the average distance between sections (cm). Muscle-tendon interface area was estimated with the formula: Interface area (mm^2) = ΣId, where I is the line of interface measured in cross-section (mm) and d the average distance between sections (mm) (Gundersen et al., 1988).

set to provide a flat surface, approximately mimicking the coronal plane in which the hamstrings lie *in vivo*. The muscles were laid on top, orientated according to their *in situ* arrangement and then encased with green jelly. The whole block of embedded tissue was serially sectioned into 10-mm slices using a commercial food slicer (C300; OMAS, Ontario, Canada), commencing just distal to the ischial tuberosity.

Muscle and tendon morphometry

Each tissue slice was photographed using a Canon PowerShot G10 Digital Compact Camera without flash, mounted on a copy-stand at a focal distance of 10 cm, with a scale bar for calibration of images (by RS). Serial images were imported to an iMac computer and analyzed in Photoshop (CS5 extended version 12.0.2 x64; Adobe Systems Incorporated, San Jose, California, USA). Muscles and tendons were outlined using the "quick selection" tool and a stack of serial binary silhouettes was created for each hamstring muscle (Fig. 1, Appendix S1). The cross-sectional area of each black silhouette was automatically calculated in ImageJ (Version 1.140; National Institutes of Health, USA) using the "threshold" tool and the interface between each tendon and its respective muscle(s) was traced and measured using the "free hand line" tool. The stacks of binary images were also used to produce three-dimensional reconstructions of the muscles and tendons using ImageJ and Amira (Version 4.1.2; Visage Imaging GmbH, Berlin, Germany).

Healthy volunteer study

Ten healthy, physically active (Pate et al., 1995) men aged 18–30 years (mean age 23 $\pm$ 2 years) with no history of a major posterior thigh injury or systemic musculo-skeletal disorder and no contraindication to MRI were consecutively recruited from the local community. Ethics approval was granted by the University of Otago Human Ethics Committee (reference: 11/079) and written informed consent was obtained.

Magnetic resonance imaging

Magnetic resonance scans were acquired using a 1.5T Signa Infinity whole-body imaging system with Excite software version 11 (General Electrical Medical Systems, Milwaukee, Wisconsin, USA). Both lower limbs were scanned concurrently with the participant supine. Axial proton density weighted scans were obtained (repetition time 1700 ms, echo time 34 ms, echo train length 7; 5 mm slice thickness with 5 mm interslice gap; 40 cm field of view; 384 $\times$ 384 matrix), extending from 4 cm proximal to the ischial tuberosity to the level of the femoral condyles using a 12 Channel HD body coil. Images were stored in digital format (DICOM files), transferred to an iMac computer, and then imported into OsiriX (Version 3.9.2, Geneva, Switzerland) which extrapolates the images between the 10-mm slices, enabling reconstruction.

Muscle and tendon morphometry

The length of the proximal tendon, MTJ, and muscle belly were measured using the same definitions as the cadaver study, except that the proximal landmark was defined as the point where the sacrotuberous ligament began to blend with the ischial tuberosity. The axial MRI series were analyzed (Fig. 1, Appendix S1) and reconstructed three-dimensionally as for the cadaver study (RS).

Statistical analyses

Data were exported to an Excel spreadsheet and means and standard deviations of all morphometric parameters calculated. Proximal tendon and MTJ lengths were standardized as a percentage of total muscle length to enable comparison between cadaver specimens. Proximal tendon and muscle volumes, and muscle-tendon interface area were calculated using Cavalieri's method (Gundersen et al., 1988) (Fig. 1). The relative force of muscle contraction at the three proximal MTJs was estimated by calculating the muscle belly volume: muscle-tendon interface area ratio.

Comparison of cadaver and MRI findings

Proximal MTJ lengths and volumes from cadavers and MRI participants were compared using unpaired Student's *t*-tests. Direct comparison of other parameters was not possible due to unavoidable differences between the selected proximal landmarks. A *P*-value of <0.05 was considered statistically significant.

Intraobserver and interobserver reliability

Repeat measures from randomly selected specimens/participants were performed blindly at least 3 weeks apart to ascertain (i) tendon and muscle length, from five lower limbs with the hamstring muscles *in situ* and MRIs of eight limbs from healthy participants; and (ii) muscle and tendon CSA and muscle-tendon interface length using axial cross-sections from three selected cadaver specimens and MRIs of six limbs from healthy participants (RS). With the exception of the measurements obtained directly from the muscles *in situ* all other parameters were independently assessed by a second investigator (SW) using OsiRix and ImageJ. Data were entered into IBM SPSS Statistics for Windows software (Version 21.0; Armonk, NY, USA: IBM Corp) and intra- and interobserver correlation coefficients (ICCs) were calculated and analyzed (Landis & Koch, 1977).

Results

Intra- and inter-rater reliability

Almost all measures demonstrated "substantial" or "almost perfect" repeatability and reproducibility (Appendix S2). Two exceptions were noted in the cadaver study, whereby repeatability for BFlh and SM muscle belly length, measured with the hamstring muscles *in situ* was poor. On MRI, both repeatability and reproducibility ranged between fair and moderate for ST free tendon and proximal tendon length, and measurements of BFlh tendon cross-sectional area demonstrated moderate agreement.

No significant differences were found between right and left measurements (assessed using two-tailed paired Student's *t*-tests) with the exception of the free proximal tendon of BFlh, which was on average 0.9 $\pm$ 0.6 cm longer on the left in the MRI study ($P = 0.03$). Pooled data were therefore used in the analysis of cadaver specimens.

Muscle and tendon morphometry

Data from the cadaver and MRI studies showed similar mean tendon and MTJ length measurements; however, variation was evident between individuals (Table 1). Tendon and muscle volumes differed markedly (Table 2); mean muscle belly volumes were more than three times greater in young active men than elderly male cadavers ($P < 0.001$). In both groups, SM had the longest mean proximal tendon and MTJ (the latter extending more than 20 cm), the greatest mean proximal tendon and muscle belly volumes, and the greatest mean proximal muscle-tendon interface area (84.6 cm^2); this resulted in the smallest muscle belly volume to muscle-tendon interface area ratio among the hamstring muscles. These architectural parameters were the smallest for ST with values for BFlh being intermediate between SM and ST (Tables 1 and 2). The resolution of the axial MRI images did not permit accurate muscle-tendon interface area measurements.

The morphology of the proximal tendons and MTJs were well demonstrated by three-dimensional reconstruction and was remarkably similar in elderly cadavers and young active men. Reconstructions developed from MRI scans were sharper (Fig. 2).

Proximal hamstring morphology

Biceps femoris long head and semitendinosus

In cadavers and young men, the common tendon of BFlh and ST commenced as a thick crescent on the upper medial facet of the ischial tuberosity (Fig. 3), in continuity with the sacrotuberous ligament superomedially (Appendix S3). A thin medial projection of the common tendon along the deep (anterior) surface of the proximal part of ST gave it a comma shape in proximal axial cross-sections. Distally, the medial projection separated off to form a flat tendon on the deep surface of ST, while the rest of the tendon became approximately crescentic in shape, with the muscle fibers of BFlh arising from the lateral surface. The posterior half of the crescent formed a septum between the BFlh and ST muscle fibers. After BFlh and ST separated, the tendon of BFlh became entirely intramuscular, the anterior part being integrated into the muscle belly more proximally than the posterior part. Further distally, the intramuscular tendon became thin and only minor variations in its axial cross-sectional shape were noted (Fig. 3).

The muscle fibers of ST had three, incompletely distinct areas of proximal attachment: to the medial (rounded) surface of the comma-shaped common

Table 1. Proximal hamstring muscle-tendon lengths in male cadaver specimens ($n = 10$) and young active men ($n = 10$; magnetic resonance imaging)

Muscle	Study	Length (cm)					Length ratio (%)	
		Mean (SD)					Mean (SD)	
		Range					Range	
		Proximal tendon	Proximal free tendon	Proximal MTJ	Muscle	Muscle belly	Proximal tendon/muscle	Proximal MTJ/muscle
BFlh	Cadaver	25.7 (2.9) 20.0–29.1	7.4 (1.1) 5.7–9.5	18.4 (2.5) 13.3–21.9	45.6 (2.9) 41.6–50.4	34.2 (2.3) 32.0–37.9	56.5 (5.5) 43.4–63.5	40.3 (4.9) 29.0–46.0
	MRI	26.1 (2.6) 19.6–29.2	6.4 (1.6)* 3.4–9.4	19.7 (2.6) 14.8–24.5	–	29.0 (1.4)† 25.9–31.0	–	–
ST	Cadaver	15.0 (2.1) 11.4–17.8	2.2 (0.9) 0.9–3.6	12.8 (2.0) 10.0–15.9	45.8 (3.0) 41.9–50.5	30.5 (3.7) 27.4–37.4	32.7 (3.9) 27.0–37.0	27.9 (3.6) 23.0–34.0
	MRI	11.9 (3.8) 6.6–20.5	1.1 (0.5) 0.2–2.2	10.8‡ (3.6) 5.8–19.4	–	29.6 (3.1) 24.4–36.4	–	–
SM	Cadaver	33.6 (2.0) 30.3–36.7	11.1 (1.6) 8.1–12.6	22.5 (1.2) 21.4–25.7	45.8 (3.0) 41.9–50.5	28.7 (2.4) 25.5–33.0	73.3 (1.7) 70.0–75.0	49.1 (2.7) 45.0–54.0
	MRI	31.7 (1.6) 29.4–34.2	11.2 (1.7) 7.0–14.7	20.5 (2.2) 16.1–24.6	–	25.8 (2.7)§ 23.0–28.1	–	–

The proximal landmarks for measurements were the prominent tubercle on the lateral aspect of the medial portion of the ischial tuberosity (cadavers) and the point at which the sacrotuberous ligament began to blend on the ischial tuberosity (MRI).

*Proximal free tendon was 0.9 ± 0.6 cm longer on the left ($P = 0.03$).

†Data missing for 2/10 participants as the muscle belly continued out of the field of view on MRI.

‡Quantifies attachment to the semitendinosus part of the common tendon; (–) Demarcates where length or ratio measurements were not available due to field of view limitations (muscle length).

§Data missing for 8/10 participants as the muscle belly continued out of the field of view on MRI.

BFlh, biceps femoris long head; MRI, magnetic resonance imaging; MTJ, musculo-tendinous junction; SD, standard deviation; SM, semimembranosus; ST, semitendinosus.

Table 2. Proximal hamstring muscle-tendon volumes and interface area in male cadaver specimens ($n = 10$) and young active men ($n = 10$; magnetic resonance imaging)

Muscle	Study	Volume (cm^3)		Muscle-tendon interface area (cm^2)	Muscle belly volume/interface ratio
		Mean (SD)		Mean (SD)	
		Range		Range	
		Proximal tendon	Muscle belly	Proximal MTJ	Proximal MTJ
BFlh	Cadaver	5.9 (2.1) 3.5–9.8	75.8 (19.1) 51.2–109.9	45.0 (7.8) 34.5–57.3	1.68
	MRI	9.2 (3.0) 5.3–17.0	263.6 (30.0)* 225.8–314.3	–	–
ST	Cadaver	–	62.2 (17.1) 36.4–91.9 31.1 (8.8) prox 14.8–43.2	18.8 (3.7) 14.0–24.2	3.30 1.70
	MRI	–	243.3 (32.7) 185.8–302.1	–	–
SM	Cadaver	10.2 (2.6) 6.5–14.4	104.9 (50.6) 55.8–214.3	84.6 (31.5) 60.7–142.1	1.24
	MRI	12.4 (2.9)	324.4† (13.6) 313.2–344.3	–	–

Volume and muscle-tendon interface area calculated from scaled photograph and MRI axial series utilizing Cavalieri's method. The proximal landmarks for measurements were the prominent tubercle on the lateral aspect of the medial portion of the ischial tuberosity (cadavers) and the point at which the sacrotuberous ligament began to blend on the ischial tuberosity (MRI).

*Data missing for 2/10 participants as the muscle belly continued out of the field of view on MRI.

†Data missing for 8/10 participants as the muscle belly continued out of the field of view on MRI; (–) Demarcates where measurements were not available due to the proximal tendon of ST being considered together with the common tendon (BFlh and ST, volume analysis) or low MRI resolution (muscle-tendon interface area).

BFlh, biceps femoris long head; MRI, magnetic resonance imaging; MTJ, musculo-tendinous junction; prox, proximal region of ST; SD, standard deviation; SM, semimembranosus; ST, semitendinosus.

tendon; to the flat tendon lying on the deep (anterior) surface of the muscle; and to the connective tissue covering the ischial tuberosity (Fig. 3). The intramuscular tendinous inscription of ST was visible in all cadaver specimens, forming an oblique interface between the proximal and distal muscle bellies. In cross-section, it was crescentic in shape and descended laterally and obliquely through the muscle (Appendix S4).

Semimembranosus

The proximal tendon of SM originated on the upper lateral facet of the ischial tuberosity (Appendix S4). Immediately below the ischial tuberosity, its tendon narrowed and rotated approximately 90° to lie in the coronal plane (Figs 3 and 4). Distal to this point it became almost circular, with a greater mean cross-sectional area (86.2 mm^2) than the common BFlh/ST tendon (46.8 mm^2) at the same level ($P < 0.001$). Further distally, the SM tendon demonstrated a thin, membranous projection medially, resulting in a "tadpole like" profile, with a rounded head laterally and a tail skirting the anterior surface of the SM muscle belly medially. The thin membranous medial projection of the tendon split at its medial border to accommodate the proximal muscle fibers of SM. As the muscle thickened distally the tendon became completely intramuscular (Fig. 4).

Discussion

Our study provides novel and reliable dissection and MRI data on the morphology and morphometry of the proximal tendons and MTJs of the hamstring complex, including their three-dimensional arrangement and quantification of muscle-tendon interface area relative to muscle size. Consistent with previous reports we found that the proximal tendons of SM and BFlh were expansive and characterized by long proximal MTJs, each with an extensive intramuscular course (Woodley & Mercer, 2005; Miller et al., 2007; Kellis et al., 2009; van der Made et al., 2015). With regard to morphometric parameters a consistent hierarchy was evident, with SM having the longest tendon and MTJ, the largest proximal tendon and muscle belly volume, and the greatest muscle-tendon interface area; followed by BFlh, and ST. This pattern was inverted when considering muscle belly volume to muscle-tendon interface area ratio, with SM displaying the smallest ratio, ST the largest, and BFlh being intermediary.

The majority of reported hamstring strains are located near the proximal MTJ of BFlh (Storey

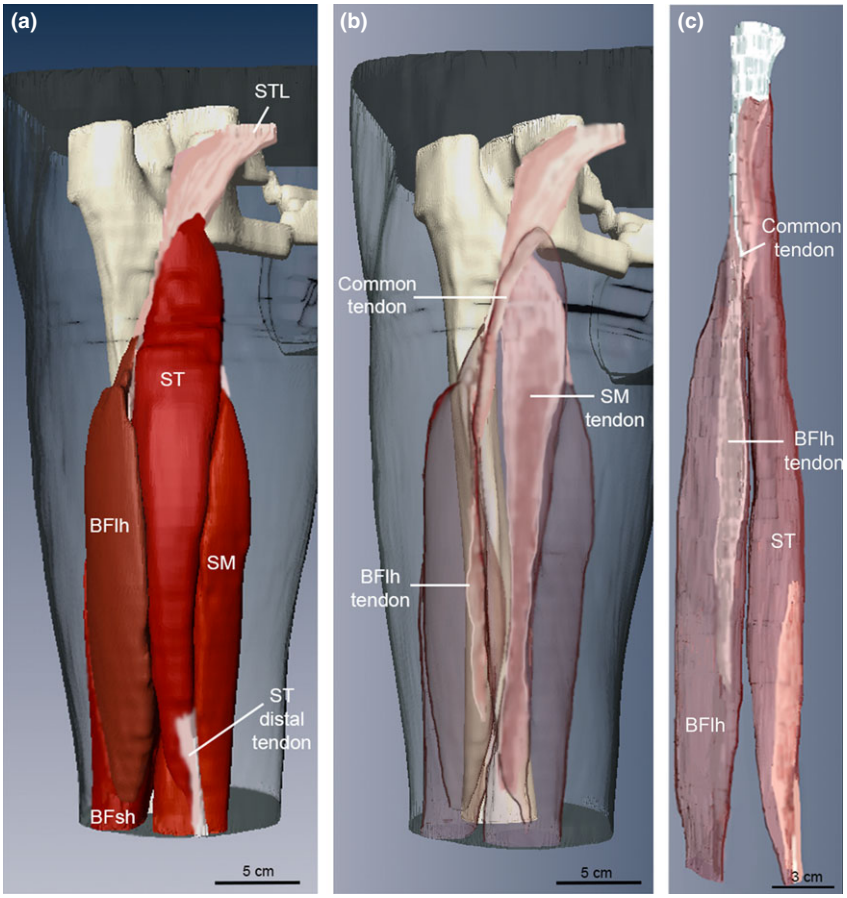

Fig. 2. Representative three-dimensional reconstruction of the hamstring muscles and proximal tendons from axial magnetic resonance images of a physically active, 22-year-old male (a and b) and serial sectioning in an elderly male cadaver (c), posterior view. Note that in Fig. 1b and c the muscle bellies are transparent to show the morphology of the intramuscular tendons. Due to MRI artifact, Fig. 1b and c are representative rather than absolute reconstructions of tendon and muscle morphology. BFlh, biceps femoris long head; BFsh, biceps femoris short head; SM, semimembranosus; ST, semitendinosus; STL, sacrotuberous ligament.

et al., 2012), meaning particular emphasis has been placed on this muscle in an attempt to explain its susceptibility to acute injury. We were interested in determining muscle-tendon interface area and its relationship with muscle belly volume (an estimate of muscle power) as it is plausible that this may influence injury, with the interface representing the area over which muscle contraction and stretch forces are dissipated. As the MTJ is a point of force concentration due to differences in compliance between the muscle and tendon fibers (Silder et al., 2010), a MTJ with a greater interface area is presumably more effective in transferring contractile forces to the bone and may be less likely to fail. We found that the muscle-tendon interface area of BFlh was intermediary to that of SM (largest) and ST (smallest). The relatively narrow (Fiorentino et al., 2012) or small (Evangelidis et al., 2015) size of the BFlh proximal aponeurosis has been suggested as a risk factor for injury, and although our data suggest that ST may be the most susceptible to injury (smallest muscle-tendon interface area, and largest muscle volume to interface area ratio), it is important to consider that ST also has several alternative routes for force dissipation from muscle contraction (discussed below). In contrast, BFlh has a single interface for force dissipation from its muscle belly and could therefore be at a mechanical disadvantage, particularly during powerful movements such as sprinting.

Information on muscle size is useful in terms of assessing morphological changes associated with injury, pathology, or in response to rehabilitation programs (Mersmann et al., 2015), yet little data are currently available on hamstring muscle cross-sectional area and volume, particularly from living individuals. This parameter is also relevant because, as discussed above, the volume of a muscle predicts how much external work it may exert on its proximal MTJ (O'Brien et al., 2009). Biceps femoris long head (active young men, mean volume 263.6 $\pm$ 30.0 cm^3) was larger than ST (243.3 $\pm$ 32.7 cm^3), yet considerably smaller than SM (324.4 $\pm$ 13.6 cm^3). This hierarchy is consistent with another MRI study (Tate

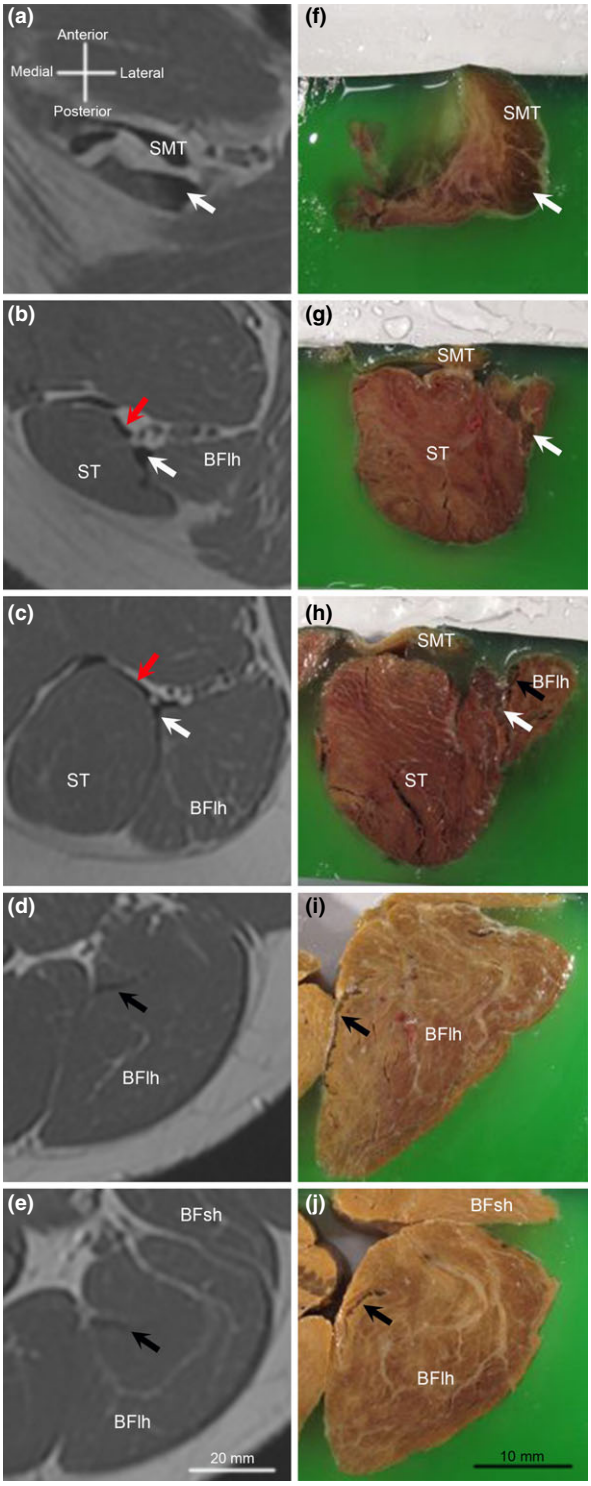

Fig. 3. Cross-sections of biceps femoris long head and semitendinosus, from axial magnetic resonance images of a physically active 22-year-old male (a–e) and serial sectioning in an elderly male cadaver (f–j), from proximal (a and f) extending distally at regular intervals. Of note is the course and morphology of the common tendon (white arrows) which continues as the proximal intramuscular tendon of BFlh (black arrows), and the additional proximal tendon of ST on the anterior surface of its muscle belly (red arrows). BFlh, biceps femoris long head; BFsh, biceps femoris short head; SMT, semimembranosus tendon; ST, semitendinosus.

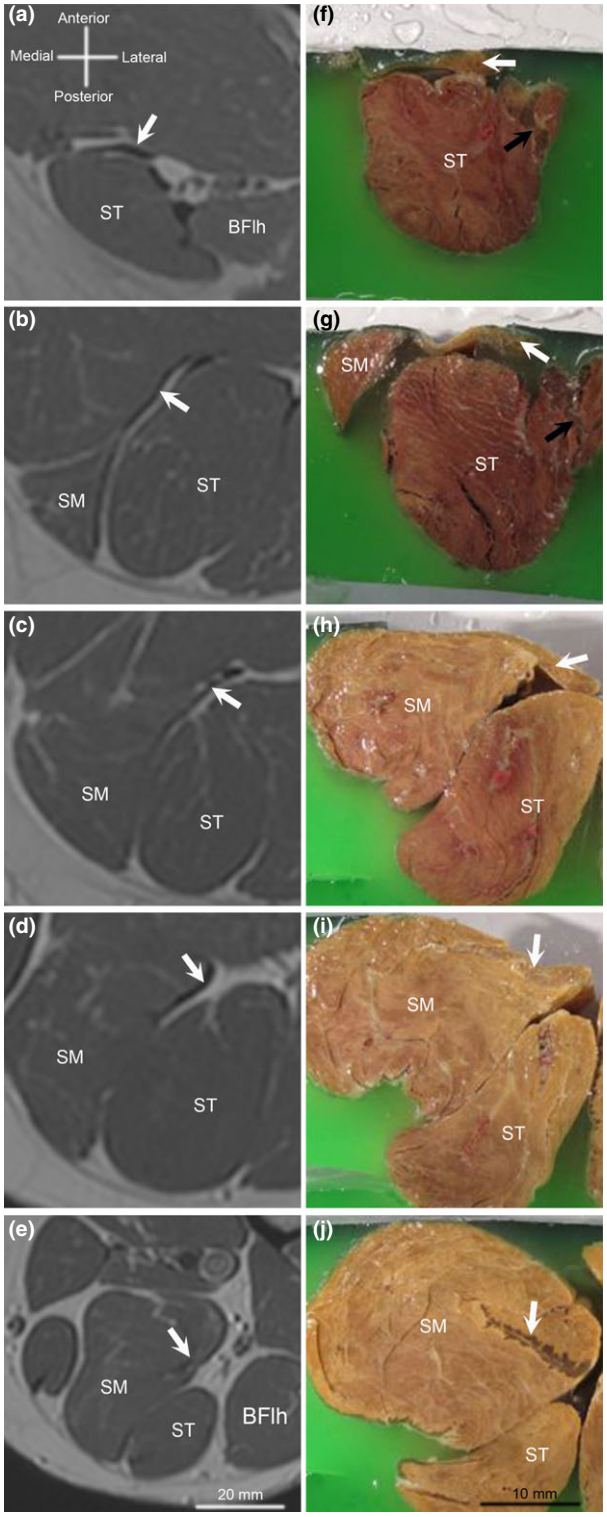

Fig. 4. Cross-sections of semimembranosus and semitendinosus, from axial magnetic resonance images of a physically active 22-year-old male (a–e) and serial sectioning in an elderly male cadaver (f–j), distal to the ischial tuberosity extending distally at regular intervals. Of note is the course and morphology of the semimembranosus tendon (white arrows) and the common tendon proximal intramuscular tendon of BFlh and ST (black arrows). BFlh, biceps femoris long head; SM, semimembranosus; ST, semitendinosus.

et al., 2006), although our participants demonstrated larger muscle bulks than have been previously reported (Tate et al., 2006; Evangelidis et al., 2015), likely due to differences in participant age and activity levels. Interestingly, the participants in the study by Tate et al. (2006) were approximately 4 years younger than those in our study but were similarly active, suggesting that BFlh muscle belly volume increases by approximately 30% between late teenage years and the early 20s in physically active men. Although one study reported no relationship between BFlh muscle size or strength and proximal muscle-tendon interface area (Evangelidis et al., 2015), further investigation of proximal morphology in a larger sample, taking into consideration the entire hamstring complex alongside functional and clinical parameters, seems warranted.

Strains involving ST are less frequent that those affecting BFlh (Slavotinek et al., 2002), and while they may present in isolation they predominantly occur simultaneously with BFlh injuries (Storey et al., 2012), presumably due to the same mechanism. The precise anatomical location(s) of ST injuries are generally not well defined (Storey et al., 2012), but a recent account of lesions in footballers shows that the proximal muscle belly is more frequently affected (15.3%) than the proximal MTJ (2%) or tendon (2.3%) (Crema et al., 2015). Semitendinosus is characterized by its intramuscular tendinous inscription which divides the muscle into proximal and distal regions. This may serve to provide added muscle-tendon interface area for its muscle fibers, which is also available via an additional proximal tendinous connection to the ischial tuberosity (as well as through the common tendon). Although our muscle-tendon data suggest that ST may be the most prone of all the hamstrings to injury, it is possible that these unique structures reduce the force concentration at its proximal MTJ, meaning this area is less susceptible to injury.

The prevalence of SM strains is on par with those affecting ST (Storey et al., 2012) and sports such as football can give rise to SM injuries, usually at the proximal MTJ (Crema et al., 2015). However, SM appears to be injured frequently during slow speed stretching activities (Storey et al., 2012), which are predominantly reported among dancers, especially during sagittal splits. In these instances, the majority of strain injuries are located at the proximal free tendon rather than the MTJ (Askling et al., 2007b, 2008). As suggested by Askling et al. (2007b, 2008), a relationship may exist between the injury situation and muscle-tendon involvement; therefore, we hypothesize that the length of the free tendon of SM, its spiral course, and medial thickness may render it vulnerable to stretch injuries. Its long proximal tendon attaches high on the lateral facet of the ischial tuberosity and continues distally and medially in the thigh; this arrangement will predispose to significant stretch, particularly during extreme ranges of movement when the muscle is extended across both the knee and hip joints.

Semimembranosus had the largest muscle volume but, in direct contrast to its proximal tendon length, the shortest muscle belly in both male cadavers and young active men. As a result of this distinctive architecture, SM displayed the greatest muscle-tendon interface area (nearly double that of BFlh, and over four times greater than that of ST), and the lowest muscle belly to muscle tendon interface area ratio. These morphological findings suggest that the power produced by this large muscle is dissipated over an extensive muscle-tendon interface area resulting in the least amount of force concentration at the proximal MTJ.

Three-dimensional reconstruction of the hamstrings in particular serves to highlight the extent of the proximal tendons and integration of the MTJs of BFlh and SM within their respective muscle bellies. Understanding this morphology and potential variation is important in clinical and radiological diagnoses of hamstring strain injury, as accurate classification and grading of muscle-tendon injuries are reliant on detailed anatomical descriptions (Hamilton et al., 2015). In our study, mean tendon and MTJ lengths were similar between cadavers and active young men, but it is worth noting that these were highly variable between individuals, as was tendon and muscle belly volume and muscle-tendon interface area. This variation possibly adds complexity to determining location of injury, and while the morphology of injury is attracting greater attention (Comin et al., 2013; Crema et al., 2015), it would be interesting to further explore three-dimensional morphometric parameters and injury patterns using research tools such as diffusion tensor imaging (Oudeman et al., 2015).

Our study has some limitations. Our results are based on dissection of male elderly cadavers and MRI scans of physically fit young men. The focus on men reflects the overall gender bias observed in hamstring strains (Slavotinek et al., 2002; Koulouris & Connell, 2003; Connell et al., 2004), but it would be important to also examine hamstring architecture in females. Anatomical findings in embalmed elderly cadavers may be altered by muscle atrophy and tissue shrinkage following fixation (Cutts, 1988), and as anticipated the mean muscle volumes in elderly cadavers was substantially smaller than that in young active mean. However, the overall architecture of the MTJ is not likely to be markedly altered and all the hamstrings would be similarly affected, allowing comparison between muscles. Magnetic resonance imaging was limited by the field of view,

reducing the sample sizes for muscle belly length and volume measurements, particularly for SM. The resolution of MR scans prevented accurate measurement of the muscle-tendon interface at the MTJ and also impacted on three-dimensional reconstruction, which should be considered representative of muscle-tendon morphology rather than an absolute model.

In conclusion, this study emphasizes the morphological differences between the proximal hamstring muscles in men and provides novel three-dimensional images of the MTJs. The proximal MTJ anatomy of each muscle was variable between individuals but mean values were relatively constant between elderly male cadavers and physically active young men. A hierarchy for total proximal tendon, free tendon, and MTJ lengths was apparent, with SM having the longest tendon, followed by BFlh and ST. This may render SM more prone to stretching injuries than BFlh and ST. Although the ratio of muscle belly volume to muscle-tendon interface area was greatest for ST, other anatomical factors may offset force concentration at the proximal MTJ of ST, making BFlh the most vulnerable to proximal hamstring strains.

Perspective

Knowledge of hamstring muscle architecture, including an appreciation of proximal muscle-tendon architecture, is fundamental to understanding hamstring strain injury. Findings from this study demonstrate that morphological differences exist between the proximal hamstring muscles in men, and that the anatomy of the proximal muscle-tendon complex may be variable between individuals. Specific architectural features such as proximal MTJ morphology, and muscle belly volume to muscle-tendon interface area could be relevant when considering the susceptibility of each muscle to injury. Further exploration of the anatomy of the proximal MTJ in larger samples of healthy individuals, with and without a history of hamstring injury, might improve our understanding of the pathoanatomical basis and distribution of acute hamstring strains, which could ultimately lead to better diagnostic, therapeutic, and preventive strategies.

Key words: Muscle, skeletal, tendons, dissection, magnetic resonance imaging.

Acknowledgements

We express our gratitude to those who selflessly donated their bodies for anatomic study and research, and to the young men who participated in this study. We thank the staff in the Radiology Department, Dunedin Public Hospital for assisting with the MRI and to Robbie McPhee for helping produce Fig. 1. No external financial support was received for this project.

Contributors

RNS, MDS, and SJW were responsible for the conception and design of the study, and had full access to all the data. RNS coordinated the study and collected the data. GM was the radiologist involved in assisting with the MRI and contributed to the analysis of this aspect of the project. RNS wrote the first draft of the manuscript, SJW managed the process from first to final draft, and all authors provided feedback on the article and contributed to the final version of the manuscript. All authors have read and approved the final submission.

Competing interests

None.

References

Askling CM, Saartok T, Thorstensson A. Type of acute hamstring strain affects flexibility, strength, and time to return to pre-injury level. Br J Sports Med 2006: 40: 40–44.

Askling CM, Tengvar M, Saart T, Thorstensson A. Sports related hamstring strains – two cases with different etiologies and injury sites. Scand J of Med Sci Sports 2000: 10: 304–307.

Askling CM, Tengvar M, Saartock T, Thorstensson A. Acute first-time hamstring strains during high-speed running: a longitudinal study including clinical and magnetic resonance imaging findings. Am J Sports Med 2007a: 35: 197–205.

Askling CM, Tengvar M, Saartok T, Thorstensson A. Acute first-time hamstring strains during slow-speed stretching: clinical, magnetic resonance imaging, and recovery characteristics. Am J Sports Med 2007b: 35: 1716–1724.

Askling CM, Tengvar M, Saartock T, Thorstensson A. Proximal hamstring strains of stretching type in different sports. Am J Sports Med 2008: 36: 1799–1904.

Battermann N, Appell HJ, Dargel J, Koebke J. An anatomical study of the proximal hamstring muscle complex to elucidate muscle strains in this region. Int J Sports Med 2011: 32: 211–215.

Chleboun GS, France AR, Crill MT, Braddock HK, Howell JN. In vivo measurement of fascicle length and pennation angle of the human biceps femoris muscle. Cells Tissues Organs 2001: 169: 401–409.

Comin J, Malliaras P, Baquie P, Barbour T, Connell D. Return to competitive play after hamstring injuries involving disruption of the central tendon. Am J Sports Med 2013: 41: 111–115.

Connell D, Schneider-Kolsky ME, Hoving JL, Malara F, Buchbinder R, Koulouris G, Burke F, Bass C. Longitudinal study comparing sonographic and MRI assessments of acute and healing hamstring injuries. Am J Roentgenol 2004: 183: 975–984.

Crema MD, Guermazi A, Tol JL, Niu J, Hamilton B, Roemer FW. Acute hamstring injury in football players:

association between anatomical location and extent of injury – a large single-center MRI report. J Sci Med Sport 2015: doi: 10.1016/j.jsams.2015.04.005

Cutts A. Shrinkage of muscle fibres during the fixation of cadaveric tissue. J Anat 1988: 160: 75–78.

De Smet AA, Best TM. MR imaging of the distribution and location of acute hamstring injuries in athletes. Am J Roentgenol 2000: 174: 393–399.

Eirale C, Farooq A, Smiley FA, Tol JL, Chalabi H. Epidemiology of football injuries in Asia: a prospective study in Qatar. J Sci Med Sport 2013: 16: 113–117.

Evangelidis PE, Massey GJ, Pain MT, Folland JP. Biceps femoris aponeurosis size: a potential risk factor for strain injury? Med Sci Sports Exerc 2015: 47: 1383–1389.

Fiorentino NM, Epstein FH, Blemker SS. Activation and aponeurosis morphology affect in vivo muscle tissue strains near the myotendinous junction. J Biomech 2012: 45: 647–652.

Garrett WE, Rich FR, Nikolaou PK, Vogler JB. Computed tomography of hamstring muscle strains. Med Sci Sports Exerc 1989: 21: 506–514.

Gibbs NJ, Cross TM, Cameron M, Houang MT. The accuracy of MRI in predicting recovery and recurrence of acute grade one hamstring muscle strains within the same season in Australian Rules football players. J Sci Med Sport 2004: 7: 248–258.

Gundersen H, Bendtsen L, Korobo L, Marcussen N, Moller A, Nielsen K, Nyengaard J, Pakkenberg B, Sorensen F, Vesterby A, West M. Some new, simple and efficient stereological methods and their use in pathological research and diagnosis. APMIS 1988: 96: 379–394.

Hamilton B, Valle X, Rodas G, Til L, Grive RP, Rincon JA, Tol JL. Classification and grading of muscle injuries: a narrative review. Br J Sports Med 2015: 49: 306.

Kellis E, Galanis N, Natsis K, Kapetanos G. Validity of architectural properties of the hamstring muscles: correlation of ultrasound findings with cadaveric dissection. J Biomech 2009: 42: 2549–2554.

Koulouris G, Connell D. Evaluation of the hamstring muscle complex following acute injury. Skeletal Radiol 2003: 32: 582–589.

Landis JR, Koch GG. The measurement of observer agreement for categorical data. Biometrics 1977: 33: 159–174.

Mendiguchia J, Alentorn-Geli E, Brughelli M. Hamstring strain injuries: are we heading in the right direction? Br J Sports Med 2012: 46: 81–85.

Mersmann F, Bohm S, Schroll A, Boeth H, Duda G, Arampatzis A. Muscle shape consistency and muscle volume prediction of thigh muscles. Scand J Med Sci Sports 2015: 25: e208–e213.

Miller SL, Gill J, Webb GR. The proximal origin of the hamstrings and surrounding anatomy encountered during repair. A cadaveric study. J Bone Joint Surg 2007: 89: 44–48.

O'Brien TD, Reeves ND, Baltzopoulos V, Jones DA, Maganaris CN. Strong relationships exist between muscle volume, joint power and whole-body external mechanical power in adults and children. Exp Physiol 2009: 94: 731–738.

Orchard JW, Seward H, Orchard JJ. Results of 2 decades of injury surveillance and public release of data in the Australian Football League. Am J Sports Med 2013: 41: 734–741.

Oudeman J, Nederveen AJ, Strijkers GJ, Maas M, Luijten PR, Froeling M. Techniques and applications of skeletal muscle diffusion tensor imaging: a review. J Magn Reson Imaging 2015: doi:10.1002/jmri.25016.

Pate RR, Pratt M, Blair SN, Haskell WL, Macera CA, Bouchard C, Buchner D, Ettinger W, Heath GW, King AC, Kriska A, Leon AS, Marcus BH, Morris J, Paffenbarger RS, Patrick K, Pollock ML, Rippe JM, Sallis J, Wilmore JH. Physical activity and public health: a recommendation from the Centers for Disease Control and Prevention and the American College of Sports Medicine. J Am Med Assoc 1995: 305: 1061–1154.

Petersen J, Thorborg K, Nielsen MB, Holmich P. Acute hamstring injuries in Danish elite football: a 12-month prospective registration study among 374 players. Scand J Med Sci Sports 2010: 20: 588–592.

Petersen J, Thorborg K, Nielsen MB, Skjodt T, Bolvig L, Bang N, Holmich P. The diagnostic and prognostic value of ultrasonography in soccer players with acute hamstring injuries. Am J Sports Med 2014: 42: 399–404.

Sato K, Nimura A, Yamaguchi K, Akita K. Anatomical study of the proximal origin of hamstring muscles. J Orthopaed Sci 2012: 17: 614–618.

Seidel PM, Seidel GK, Gans BM, Dijkers M. Precise localization of the motor nerve branches to the hamstring muscles: an aid to the conduct of neurolytic procedures. Arch Phys Med Rehab 1996: 77: 1157–1160.

Silder A, Reeder SB, Thelen DG. The influence of prior hamstring injury on lengthening muscle tissue mechanics. J Biomech 2010: 43: 2254–2260.

Slavotinek JP, Verrall GM, Fon GT. Hamstring injury in athletes: using MR imaging measurements to compare extent of muscle injury with amount of time lost from competition. Am J Roentgenol 2002: 179: 1621–1628.

Storey RN, Stringer MD, Woodley SJ. Site of acute hamstring strains and activities associated with injury: a systematic review. NZ J Sport Med 2012: 39: 36–42.

Tate CM, Williams GN, Barrance PJ, Buchanan TS. Lower extremity muscle morphology in young athletes: an MRI-based analysis. Med Sci Sports Exerc 2006: 38: 122–128.

van der Made AD, Wieldraaijer T, Kerkhoffs GM, Kleipool RP, Engebretsen L, van Dijk CN, Golano P. The hamstring muscle complex. Knee Surg Sports Traumatol Arthrosc 2015: 23: 2115–2122.

Wickiewicz TL, Roy RR, Powell PL, Edgerton VR. Muscle architecture of the human lower limb. Clin Orthop Relat Res 1983: 179: 275–283.

Woodley SJ, Mercer SR. Hamstring muscles: architecture and innervation. Cells Tissues Organs 2005: 179: 125–141.